

# A Resolved Circumstellar Disk around the Herbig Ae Star HD 100546 in the Thermal Infrared

Wilson M. Liu<sup>1</sup>, Philip M. Hinz<sup>1</sup>, Michael R. Meyer<sup>1</sup>, Eric E. Mamajek<sup>1</sup>, and William F. Hoffmann<sup>1</sup>, and Joseph L. Hora<sup>2</sup>

## ABSTRACT

We present mid-infrared nulling interferometric and direct imaging observations of the Herbig Ae star HD 100546 obtained with the Magellan I (Baade) 6.5 m telescope. The observations show resolved circumstellar emission at 10.3, 11.7, 12.5, 18.0, and 24.5  $\mu\text{m}$ . Through the nulling observations (10.3, 11.7 and 12.5  $\mu\text{m}$ ), we detect a circumstellar disk, with an inclination of  $45 \pm 15$  degrees with respect to a face-on disk, a semimajor axis position angle of  $150 \pm 10$  degrees (E of N), and a spatial extent of about 25 AU. The direct images (18.0 and 24.5  $\mu\text{m}$ ) show evidence for cooler dust with a spatial extent of 30-40 AU from the star. The direct images also show evidence for an inclined disk with a similar position angle as the disk detected by nulling. This morphology is consistent with models in which a flared circumstellar disk dominates the emission. However, the similarity in relative disk size we derive for different wavelengths suggests that the disk may have a large inner gap, possibly cleared out by the formation of a giant protoplanet. The existence of a protoplanet in the system also provides a natural explanation for the observed difference between HD 100546 and other Herbig Ae stars.

*Subject headings:* stars: individual (HD 100546)—stars: pre-main sequence—techniques: interferometric

## 1. Introduction

Circumstellar disks provide insight into the formation of planetary systems. These disks are observed most readily around luminous pre-main-sequence (PMS) stars. Herbig

---

<sup>1</sup>Steward Observatory, University of Arizona, 933 N. Cherry Ave., Tucson, AZ, USA 85721, e-mail: wliu@as.arizona.edu

<sup>2</sup>Harvard-Smithsonian Center for Astrophysics, 60 Garden St., MS 42, Cambridge, MA, USA 02138

Ae (HAE) stars, the evolutionary precursors to intermediate mass main-sequence stars such as Vega, have been identified to have infrared (IR) excess emission. The source of the emission has been hypothesized by Hillenbrand et al. (1992) and Lada & Adams (1992) to originate from a geometrically thin, optically thick circumstellar disk, with an optically thin inner region and a high accretion rate in order to explain the observed spectral energy distribution (SED) of such stars. An alternative interpretation suggests that the emission may be a result of a "dusty nebula" (or envelope), rather than a disk (Hartmann, Kenyon, & Calvet 1993). Recent modelling has shown a likely possibility to be a disk which flares vertically with increasing radius from the star (Chiang & Goldreich 1997; Kenyon & Hartmann 1987). Other studies have found that these disks may have a more complex structure, incorporating an inner hole and heating of the inner wall of the disk to account for an excess in near-IR emission (Dullemond, Dominik, & Natta 2001). Another model incorporates an extended spherical envelope surrounding a thin disk (Miroshnichenko et al. 1999). We refer the reader to Natta, Grinin, & Mannings (2000) for an extensive review of recent results. In general, observations of the circumstellar environments of PMS stars are an important step in determining which models are most representative of their true environment, as well as understanding the evolution of protoplanetary disks into planetary systems.

The nearby ( $\sim 100$  pc) HAE star HD 100546 has been the focus of several studies. Malfait et al. (1998) characterized the spectrum of the star in the IR, and identified several spectral features indicative of silicate and polycyclic aromatic hydrocarbon (PAH) species in the circumstellar environment. They also found features in the spectrum of HD 100546 to be very similar to those in comet Hale-Bopp, indicating the presence of cometary material in the system, and hypothesize that the system could harbor giant protoplanets to explain the presence of crystalline silicates in the cometary material. A recent study by Bouwman et al. (2003) found the spectrum of HD 100546 to be dramatically different from other HAE stars, and propose a model with a circumstellar disk with an inner gap of 10 AU and a giant protoplanet. Three studies, Grady et al. (2001); Augereau et al. (2001) and Pantin, Waelkens, & Lagage (2000), used coronagraphic observations at near-IR wavelengths to image the dust disk in scattered light and characterize its spatial structure. These studies detect evidence of an inclined dust disk, and are in good agreement as to its inclination ( $\approx 40^\circ$  from face-on), and position angle of its semimajor axis ( $130^\circ$  to  $160^\circ$  E of N). Extended emission has also been detected at 3.4 mm (Wilner et al. 2003), and far-ultraviolet observations of warm molecular hydrogen are also consistent with the presence of an inclined disk (Lecavelier des Etangs et al. 2003). The presence of circumstellar emission from HD 100546, as well as its relative proximity, make it an ideal target for nulling interferometry.

Nulling interferometry is a technique used to study circumstellar environments by suppressing the starlight which normally overwhelms any signal from the faint circumstellar

material. The technique is implemented by overlapping the pupils of two telescopes (or two subapertures from a single telescope) with an appropriate path length difference to destructively interfere the light. The result is a sinusoidal transmission pattern where the unresolved central point source is suppressed and the surrounding resolved structure can be detected.

In this Letter, we present the results of nulling interferometric and direct imaging observations of the HAE star HD 100546 in the mid-IR. We discuss the detection and structure of resolved emission surrounding the star at several wavelengths. For further background we refer the reader to Hinz, Hoffmann, & Hora (2001).

## 2. Observations & Data Reduction

Observations were made in August 2001 and May 2002 at the Magellan I (Baade) 6.5 m telescope at Las Campanas Observatory near La Serena, Chile. The Bracewell Infrared Nulling Cryostat (BLINC) was the nulling interferometer used to provide suppression of starlight, creating an interferometer with two 2.5 m subapertures and a baseline of 4 m. The Mid-InfraRed Array Camera (Hoffmann et al. 1998, MIRAC) provided the final stop for the two beams of the interferometer. Nulling observations were taken at 10.3, 11.7 and 12.5  $\mu\text{m}$  with 10% bandpass at each wavelength. Images of the science object, HD 100546, were taken at seven different rotations of the interferometer baseline with respect to the sky in order to probe the geometry of the circumstellar dust (discussed in Section 3.1). Thirty-seven sets of 500 frames were taken (2 sets at each combination of wavelength and rotation for all but one of the combinations), each frame with an integration time of 0.5 s. These observations were interlaced with observations of calibrator stars, with the same integration times. Frames were sky subtracted using off-source sky frames taken in between observations. A custom IDL program was used to perform aperture photometry on each image and pick out, for each set of 500 frames, the image with the best instrumental null.

Direct images at 11.7, 18.0 and 24.5  $\mu\text{m}$  were obtained in August 2001 and March 2003. Images were taken with a 3 Hz chop of 8'' in the horizontal direction of the detector, and a nod of 8'' in the vertical direction after every 15 s of integration. The 11.7  $\mu\text{m}$  images were taken to verify extended emission detected by nulling, with a total integration time of 60 s. The 18.0 and 24.5  $\mu\text{m}$  images were taken with the purpose of detecting resolved material at longer wavelengths and characterizing emission from cooler dust. Total integration times were 170 s at 18.0  $\mu\text{m}$  and 210 s at 24.5  $\mu\text{m}$ . Aperture photometry was performed on the direct images of HD 100546 and calibrator stars and relative fluxes for the science object were transformed to absolute fluxes using calibrator fluxes taken from Gezari et al. (1993). The absolute fluxes are 67 Jy at 11.7  $\mu\text{m}$ , 123 Jy at 18.0  $\mu\text{m}$ , and 165 Jy at 24.5  $\mu\text{m}$ , and

are good to 10%.

### 3. Results

#### 3.1. Nulling Observations

Table 1 shows the source nulls and errors achieved at each combination of wavelength and rotation. The source null for the science object is calculated by subtracting the null achieved on the calibrator star from the instrumental null achieved on the science object, and represents the percentage of light remaining in the image when nulled, compared to the full flux when the pupils are constructively interfered. The best source null is calculated for each set of 500 frames. The adopted values for the source null presented in Table 1 are taken to be the average of the best nulls in each of the two sets of frames taken at each combination of wavelength and rotation. The error in the null is taken to be the difference in the the best nulls in the two sets of frames.

The non-zero source nulls on HD 100546 are indicative of extended emission surrounding the star. Our results show that the source null of the object varies as a function of rotation of interferometer baseline with respect to the sky (Figure 1). At all three wavelengths, the null varies by a factor of 2 or more and appears to have roughly the same dependence. From this dependence, we can infer the presence of an inclined structure, as well as its size and orientation in the following manner. The transmitted signature of the nulling interferometer is an interference pattern with interference fringes along the baseline. If these fringes are parallel to the major axis of a disk, more of the disk’s light will be nulled, resulting in a lower percentage of remaining light. When the fringes are aligned orthogonally to the major axis, the value of the source null will be higher (i.e., there is more light remaining). Therefore, there should be a variation in null with respect to rotation of the baseline. This relation will have a sinusoidal form, with a period of  $180^\circ$  and an amplitude dependent on the projected emitting surface of the disk, and consequently its inclination. We have performed a least squares fit of such a function for the expected null (see Fig. 1),  $N = a + b * \sin(PA + \theta)$ . The value of  $a$  is a vertical offset (physically related to the size of the disk),  $b$  is the amplitude of the sine function (related to the inclination of the disk),  $PA$  is the position angle of the semimajor axis, and  $\theta$  is the rotation of the interferometer baseline relative to the sky. We find the parameters shown in Table 2 as the best fits for the data. The values derived for all three wavelengths are in agreement with one another, with average derived uncertainties in the nulls of 6.3, 5.5, and 5.5% for 10.3, 11.7, and 12.5  $\mu\text{m}$ , respectively.

In order to interpret these fits physically, we have calculated the physical parameters

which would yield these fit parameters for two simple disk distributions: an inclined Gaussian disk and a ring. Table 3 shows the best fit physical parameters for the nulling data. The best fit position angle of the semimajor axis of the disk is  $140^\circ$  to  $160^\circ$  (E of N), which is in agreement with the values derived from near-IR coronagraphic studies (Grady et al. 2001; Augereau et al. 2001; Pantin, Waelkens, & Lagage 2000). The inclination of the disk at 10.3 and 11.7  $\mu\text{m}$  is derived to be  $30^\circ$  to  $40^\circ$  from face-on, also in agreement with the aforementioned studies, but these fits are only marginally better than a face-on disk when comparing the reduced  $\chi^2$  ( $= 1.5$  and  $2.2$  for the 10.3 and 11.7  $\mu\text{m}$  fits, respectively) of the fits. The 12.5  $\mu\text{m}$  data show a larger amplitude in the variation of the null, hence the inclination derived is greater,  $\approx 60^\circ$  from face-on. In this case, there is significant inclination of the disk, as the fit yields reduced  $\chi^2 = 2.4$  as opposed to 7.5 for a face-on disk.

The multiwavelength nature of our observations also allow us to probe differences between the distribution of different species (silicates, PAH, etc.) and the thermal continuum. Our observations at 10.3  $\mu\text{m}$  and 11.7  $\mu\text{m}$  probe emission from silicates and PAH species, while the continuum emission is roughly probed by the 12.5  $\mu\text{m}$  band (Malfait et al. 1998), although the bandpass of this filter may result in significant emission from PAH and silicates. Our results indicate that the emitting structure is more inclined at 12.5  $\mu\text{m}$  than at the other two wavelengths. This suggests that emission from the thermal continuum may have a more inclined structure than the flux from emission lines of silicates and PAH.

### 3.2. Imaging

The 11.7  $\mu\text{m}$  images verify the presence of resolved emission detected in the nulling data. The images of HD 100546 show an average full-width at half-maximum (FWHM) of  $\sim 0.5''$ , while the calibrator star shows a FWHM about 20% smaller. This implies a disk size of about 30 AU, which confirms the disk sizes derived from the nulling data.

The 18.0 and 24.5  $\mu\text{m}$  direct images show evidence for extended emission as well, with the FWHM values for HD 100546 images on average about 8 - 10% larger than those of the calibrator stars. In order to determine the spatial extent of the extended emission, we constructed an artificial source by convolving an artificial face-on disk signature in the form of a two-dimensional Gaussian, with the PSF from the calibrator star. The artificial image was subtracted from the actual image of HD 100546. The width of the artificial Gaussian disk was varied in steps of 0.1 pix (equivalently 0.012'', or 1.2 AU at 100 pc). We adopt the disk size which resulted in the smallest residual when subtracted from the image of HD 100546. Figure 2 shows a typical image before and after subtractions of the artificial source, plotted with the same greyscale. The top-left image shows HD 100546 at 24.5  $\mu\text{m}$  in an

unsubtracted image. The top-right image shows the subtracted frame with the smallest residual. The center frames shows the subtraction residuals where the Gaussian disk was about 0.5 pix (FWHM) too small (left), and too large (right). Table 4 shows the results of the model fitting at each wavelength. The disk size adopted for each wavelength is the average of the sizes determined from the observations at the two epochs, with the error bars adopted as the difference in sizes derived for the two epochs.

At these wavelengths, we are probing both the thermal continuum and emission from silicates. As expected from cooler dust, the 24.5  $\mu\text{m}$  emission extends farther out than the 18.0  $\mu\text{m}$  dust. We do note the 24.5  $\mu\text{m}$  band contains a strong emission line from silicates (Malfait et al. 1998) that may contribute significantly on top of the thermal emission. The images also show that there may be evidence for an inclined disk in the subtracted images, as the best subtracted image still shows a roughly symmetric oversubtraction above and below the center of the star. In images at both wavelengths and both epochs, the residuals showed this type of symmetric structure, with peak of the positive residuals on a line orthogonal to the trough of the negative residuals (see center panels, Fig. 2). This structure in the residuals would be expected if the image of HD 100546 was slightly elliptical, perhaps as a result of a resolved inclined disk. We attempted subtractions with artificial sources incorporating an inclined (and rotated) Gaussian disk, rather than a face-on disk. The bottom panel of Figure 2 shows the outcome of this subtraction, resulting in a smaller residual than the best subtraction with a face-on disk (top-right panel). The position angle of the artificial disk was changed in steps of  $10^\circ$ , and the inclination was varied in steps of  $5^\circ$  in order to determine the orientation of the artificial disk which resulted in the smallest residual when subtracted from the image of HD 100546. The position angle of the semimajor axis was found to be between  $130^\circ$  and  $170^\circ$ , and the inclination was  $30^\circ$  to  $40^\circ$  from face-on, all roughly consistent with the orientation derived by previous studies in the near-IR (Augereau et al. 2001; Pantin, Waelkens, & Lagage 2000; Grady et al. 2001).

#### 4. Discussion

We are confident that we have resolved circumstellar emission from HD 100546 at all wavelengths probed in our observations. We wish to compare the physical parameters we have derived for this emission to current models for the circumstellar environments of Herbig Ae stars. Recent models we consider include those described in the Introduction. While observations at all three wavelengths show evidence for an inclined disk, our observations at 10.3 and 11.7  $\mu\text{m}$  are also consistent with a face-on or spherical emitting body. However, the 12.5  $\mu\text{m}$  null variation does provide convincing evidence for an inclined disk. Furthermore,

the derived sizes at these wavelengths are increasing with increasing wavelength (equivalently, decreasing temperature), as one might expect. Somewhat puzzling are the derived sizes of the 18.0 and 24.5  $\mu\text{m}$  disks. One would expect the thermal emission at these longer wavelengths to be spatially several times larger than the emission at the shorter wavelengths. If the source of the emission is a continuous flared disk, this relation would be given by  $T \sim r^{-0.5}$  (Chiang & Goldreich 1997). However, the disks at 18.0 and 24.5  $\mu\text{m}$  are only marginally larger than at shorter wavelengths. This discrepancy suggests that a continuous disk that extends all the way into the dust sublimation radius may not be an accurate model for the detected emission. Instead we prefer a model with a large inner disk gap, possibly cleared out by a giant protoplanet, as suggested in Bouwman et al. (2003). This would result in the shorter wavelength emission being detected further from the star than expected from a continuous disk, and make the relative sizes of the 10 and 20  $\mu\text{m}$  disks more similar than expected from a  $T \sim r^{-0.5}$  relation.

The detection of a disk around HD 100546 is also interesting in the context of the observations of Hinz, Hoffmann, & Hora (2001). The previous study performed nulling interferometric observations of three other HAE stars, HD 150193, HD 163296, and HD 179218 and found that none of them had resolved emission. This placed an upper limit on the size of the 10.3  $\mu\text{m}$  disk of 20 AU. This suggests that HD 100546 differs from these other PMS objects, as it appears to have a larger disk at 10.3  $\mu\text{m}$ . A disk such as the one observed around HD 100546 would have been resolvable around the three stars observed by Hinz, Hoffmann, & Hora (2001), and leads us to conclude that the physical structure and/or composition of the circumstellar environment is different in HD 100546 than the HAE stars. This result is consistent with the finding of Bouwman et al. (2003) that the SED of HD 100546 is dissimilar to that of other HAE stars. We also note that the hypothesis of giant protoplanet in the HD 100546 system would provide a natural explanation for the difference between HD 100546 and the stars observed in Hinz, Hoffmann, & Hora (2001). A full analysis of a larger sample of HAE stars is needed to confirm this conclusion, and will be presented in a future paper.

## 5. Acknowledgments

WL acknowledges support from the Michelson Graduate Fellowship. MM and EM acknowledge support through NASA contract 1224768 administered through JPL. EM also thanks the NASA Graduate Student Researchers Program (NGT5-50400) for support. The authors thank the staff of Las Campanas Observatory and the Magellan Project for wonderful support. BLINC was developed under a NASA/JPL grant for TPF. MIRAC is supported

by grant AST 96-18850 from the NSF with additional support from SAO.

## REFERENCES

- Augereau, J. C., Lagrange, A. M., Mouillet, D., & Ménard, F. 2001, *A&A*, 365, 78
- Bouwman, J., de Koter, A., Dominik, C., & Waters, L. B. F. M. 2003, *A&A*, 401, 577
- Chiang, E. I. & Goldreich, P. 1997, *ApJ*, 490, 368
- Dullemond, C. P., Dominik, C., & Natta, A. 2001, *ApJ*, 560, 957
- Gezari, D. Y., Schmitz, M., Pitts, P. S., & Mead, J. M. 1993, *Catalog of Infrared Observations*, 3rd ed., NASA Reference Publication 1294.
- Grady, C. A. et al. 2001, *AJ*, 122, 3396
- Hartmann, L., Kenyon, S. J., & Calvet, N. 1993, *ApJ*, 407, 219
- Hillenbrand, L. A., Strom, S. E., Vrba, F. J., & Keene, J. 1992, *ApJ*, 397, 613
- Hinz, P. M., Hoffmann, W. F., & Hora, J. L. 2001, *ApJ*, 561, L131
- Hoffmann, W. F., Hora, J. L., Fazio, G. G., Deutsch, L. K., & Dayal, A. 1998, *Proc. SPIE*, 3354, 647
- Kenyon, S. J. & Hartmann, L. 1987, *ApJ*, 323, 714
- Lada, C. J. & Adams, F. C. 1992, *ApJ*, 393, 278
- Lecavelier des Etangs, A. et al. 2003, *A&A*, 407, 935
- Malfait, K., Waelkens, C., Waters, L. B. F. M., Vandebussche, B., Huygen, E., & de Graauw, M. S. 1998, *A&A*, 332, L25
- Miroshnichenko, A., Ivezić, Ž., Vinković, D., & Elitzur, M. 1999, *ApJ*, 520, L115
- Natta, A., Grinin, V., & Mannings, V. 2000, *Protostars and Planets IV*, 559
- Pantin, E., Waelkens, C., & Lagage, P. O. 2000, *A&A*, 361, L9
- Wilner, D. J., Bourke, T. L., Wright, C. M., Jorgensen, J. K., van Dishoeck, E. F., Wong, T., *ApJ*, in press (astro-ph/0306399)



Table 1. Source Nulls for HD 100546

Rotation ( $^{\circ}$ )	10.3 $\mu\text{m}$	11.7 $\mu\text{m}$	12.5 $\mu\text{m}$
-80	$36.9 \pm 1.6$	$33.6 \pm 1.6$	$29.9 \pm 3.3$
-77	$33.8 \pm 5.0$	$32.8 \pm 3.3$	no data
-50	$31.3 \pm 7.0$	$19.7 \pm 3.6$	$43.2 \pm 0.9$
-24	$33.3 \pm 2.8$	$28.8 \pm 3.2$	$24.8 \pm 1.7$
+10	$21.2 \pm 8.9$	$23.2 \pm 3.3$	$20.3 \pm 1.6$
+13	$27.9 \pm 1.5$	$25.0 \pm 1.3$	no data
+40	$19.1 \pm 0.4$	$14.5 \pm 3.0$	$6.0 \pm 6.3$

Table 2. Best fit Sine Function Parameters

Parameter	10.3 $\mu\text{m}$	11.7 $\mu\text{m}$	12.5 $\mu\text{m}$
a	0.287	0.253	0.231
b	0.070	0.045	0.148
PA (E of N)	147	154	141

Table 3. Physical Parameters of Disk from Nulling Data

$\lambda$ ( $\mu\text{m}$ )	FWHM (Gaussian)	Inclination (Gaussian)	Diameter (Ring)	Incl. (Ring)
10.3	24 AU	40°	26 AU	37°
11.7	25	34	27	32
12.5	30	63	33	60

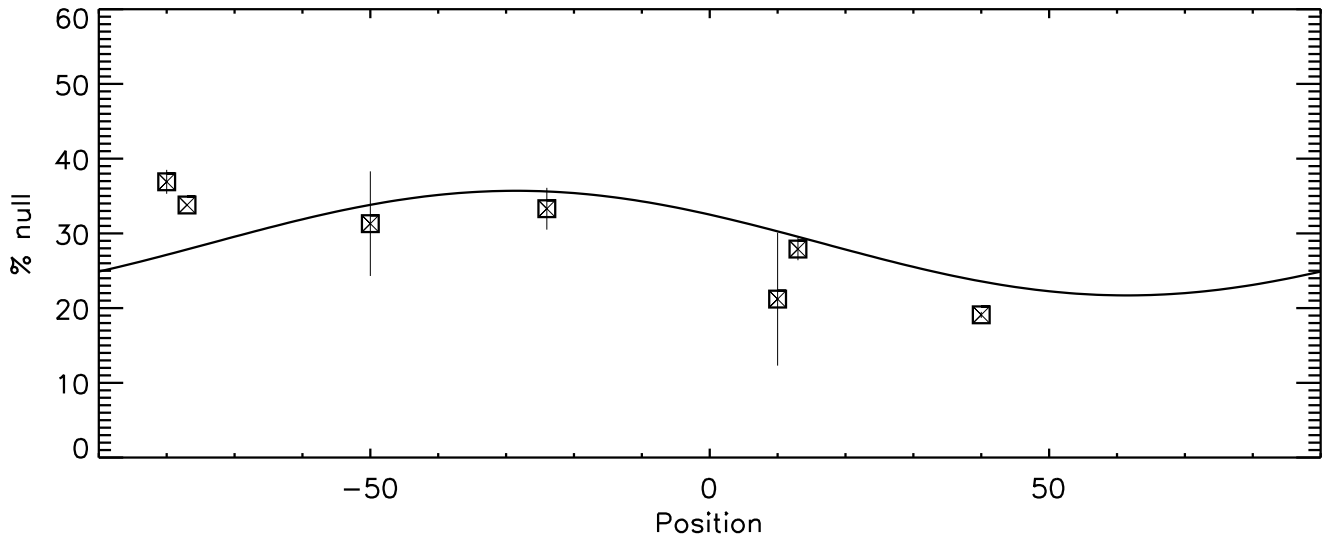
Table 4. Results from Direct Imaging

$\lambda$ ( $\mu\text{m}$ )	Disk FWHM (pix)	Angular size (arcsec)	Physical size (AU)
18.0	$2.85 \pm 0.20$	$0.34 \pm 0.02$	$34 \pm 2$
24.5	$3.55 \pm 0.20$	$0.43 \pm 0.02$	$43 \pm 2$

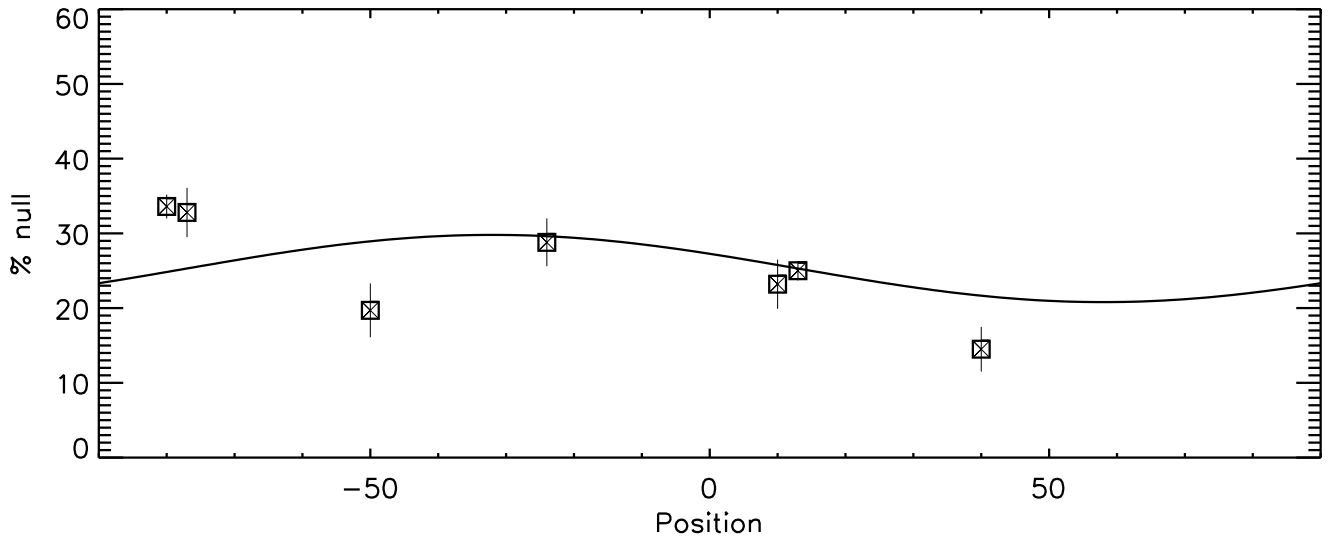
Fig. 1.— Source null vs. Rotation of the interferometer baseline for 10.3, 11.7, and 12.5  $\mu\text{m}$ .

Fig. 2.— *Top-left*: 24.5  $\mu\text{m}$  image of HD 100546, 60 s integration. *Top-right*: Residual from the best subtraction of an artificial image (with a face-on disk). *Center-left*: Residual resulting from an artificial disk 0.5 pix (FWHM) too small. *Center-right*: Residual from an artificial disk 0.5 pix too large. *Bottom*: Residual from a subtraction of an artificial source with an inclined disk.

10.3  $\mu\text{m}$  Null vs. Rotation



11.7  $\mu\text{m}$  Null vs. Rotation



12.5  $\mu\text{m}$  Null vs. Rotation

